Supplementary data

6.2.1. In vitro DPP-4, DPP-8 and DPP-9 assay

In vitro enzyme inhibitory activity was measured by fluorescence-based assay which employs fluorogenic substrate, Gly-Pro-Aminomethylcoumarin (AMC), to measure DPP (DPP-4, DPP-8 and DPP-9) activity. Cleavage of the peptide bond by DPP releases the free AMC group resulting in fluorescence that can be analyzed using an excitation wavelength of 350–360 nm and emission wavelength of 450–465 nm. The assay was performed by mixing 30 µL assay buffer (100mM/L HEPES with 0.1 mg/mL BSA, pH 7.5 for DPP-4 assay; Tris HCl 25mM and 0.1% BSA in deionized water, pH 7.5 for DPP-8 and DPP-9 assay), 10 µL of human recombinant DPP enzyme (BPS Bioscience, San Diego) and 10 µL of test compounds (of various concentrations) with 50 µL of the substrate, Gly-Pro-Amino methylcoumarin (Sigma-Aldrich). The final concentration of the DPP-4 enzyme was 1 ng/well (10 ng/well for DPP-8 and DPP-9) and of the substrate was 5 µM per well. Plates were incubated at 37 °C for 30 min kinetic run, and fluorescence was measured at excitation/emission wavelengths of 360/40, 460/40 nm at a sensitivity of 60 using a Synergy HT multi detection microplate reader (BioTek instruments). Enzyme inhibition was determined and expressed as % inhibition. The IC50 values were determined for potent compounds using Graph Pad prism software.

6.2.2. Animals

Male mice (30–35 g) were obtained from animal house of National Research Centre, Dokki, and Giza, Egypt. Rats were housed at 22 °C and 50% humidity, with a 12-hour light–dark cycle, fed a standard diet and had free access to tap water. They were kept for two weeks to acclimatize to the environmental conditions. All animals were cared for in accordance with institutional guidelines for the care and use of experimental animals.

6.2.3. Induction of diabetes

Diabetes was induced by streptozotocin, each mouse was injected intraperitoneally with a single dose of streptozotocin (65 mg/kg body weight dissolved immediately in 0.01M citrate buffer before use). After injection, mice had free access to food and water and given 5% glucose solution to drink overnight to counter hypoglycemic shock. [60, 61] After 3 days, fasting blood samples were obtained and fasting blood glucose levels were measured (> 300 mg/dl). Hyperglycemic rats were used for the experiments.

6.2.4. Experimental design

Animals were divided into 21 groups. Each group was composed of 6 rats as follows: Group one was the normal control group, group two was considered as the diabetic without receiving any tested compound and groups 3-21 were treated with the tested compounds as well as the reference drug Linagliptin.

6.2.5. Preparations of blood samples and serum

Diabetic rats were treated orally with 10 μmol/Kg body weight of different tested compounds related to the dose of standard drug (10 mg/kg body weight). Blood samples were obtained after ½, 1, 2, 3 and 26 h post treatment of the tested compounds. The blood samples were collected from each animal by scratching sub-tongual vein into sterilized tubes. Serum samples were separated by centrifugation at 3000 rpm for 10 min and used for the determination of blood glucose levels (glucose tolerance test). [60, 61]

6.3. Computational studies

6.3.1. Molecular docking methods

The crystal structure of DPP-IV (PDB: 3Wqh) was downloaded from Protein Data Bank (http://www.rcsb.org). Ligand structures were built with MOE, energy minimized using the MMFF94x force field until a RMSD gradient of 0.05 kcal was applied for all ligands. In the docking proposal the placement criterion was chosen to be Alpha Triangle, rescoring 1 was set to be London G. In this study, refinement was employed.

6.3.2. Alignment of the training set compounds

The training set compounds consisting of nine compounds of diverse chemical structures were built using the builder tool of the MOE software. The compounds were aligned using the flexible alignment tool of the program adjusting the energy cut off to 10 kcal/mol and root mean square deviation (RMSD) tolerance to 0.5. The stochastic conformation search option was applied as the method of alignment.

6.3.3. Molecular dynamics

Docked poses of compounds **7a,7f** and **7g** were used as starting point in molecular dynamics (MD) studies, the analysis was performed with MOE; 2008.10 software. Partial charges were calculated for the system and energy minimizations were done. MD was carried for 100 Pico seconds (PS)

6.3.4. Pharmacophore building

A pharmacophore model was created using the 'Pharmacophore Query Editor'. The aligned training set was used as the template for building the model. The settings of the software parameters were adjusted to: 'Unified' as the scheme of annotation 'Consensus method' for model building. Tolerance was set to 1.2 Å and the threshold was set to 75%.

6.3.5. QSAR analysis

QSAR models were performed using QSAR software of MOE 2008. The IC_{50} values were converted to PIC_{50} using equation: pIC_{50} = (-log IC_{50}), Physical descriptors, constitutional properties, topological descriptors, quantum chemical descriptors, surface area, volume and shape descriptors, and molecular properties were calculated. Predicted pIC_{50} for the data set were calculated. QSAR models were validated by applying the r^2, RMSE and residual values between expected and predicted PIC_{50}.

6.4. Radiopharmaceutical evaluation of SQ compound:

6.4.1. Radiosynthesis of ^{131}I-SQ compound

Radioiodination of SQ compound **(10a)** was achieved by the electrophilic substitution using NCA iodine-131 under oxidative conditions in the presence of chloramine-T (CAT) as an oxidizing agent [78-81]. In amber colored vials, different SQ compound amounts in DMSO were added. Then, aqueous solution of freshly prepared CAT was added followed by the addition of 10µl of ^{131}I (7.2MBq). The pH was adjusted by using 100µl of buffer solutions (4-8). The reaction mixture was vortexed and left at ambient temperature. A drop of saturated sodium metabisulfite solution (10mg/ml) was added at different time intervals to decompose the excess of iodine (I_2) in order to quench the reaction by reducing it to iodide (I^-). The radiosynthesis was optimized through the variation of pH [4-8], chloramine-T amount [100-300 µg], SQ amount [100-500 µg] and reaction time [15-120 min] to achieve the highest radiosynthesis yield. The radiosynthesis yield of ^{131}I-SQ compound was assessed by ascending paper chromatography (Whatman no. 1 - P.C.) and TLC, where one strip (1cm width and 13cm length) was used. 1–2µl of ^{131}I-SQ solution was placed 2 cm above the lower edge which allowed to evaporate spontaneously. A fresh mixture of chloroform: methanol (9:1v/v) was used for development, then, the strips were removed, dried, and cut into pieces, (1 cm length each) that were counted in a well type γ-counter. The radioiodide (I^-) remained near the origin (R_f = 0–0.1), while the ^{131}I-SQ moved with the solvent front (R_f =

0.8). Each experiment was repeated three times. One-way ANOVA was used as statistical test to evaluate data differences (level of significance set at $P<0.05$).

6.4.2. In vivo pharmacokinetic distribution of ^{131}I-SQ compound

Egyptian Atomic Energy Authority animal ethics committee regulations were followed. ^{131}I-SQ solution containing radioactivity of 8 MBq was injected I.V. in normal mice. At different time intervals post injection [15-180 min], mice were anaesthetized and dissected. All body organs and fluids of each mice were separated, and assessed for their radioactivity uptakes using NaI gamma detector. Muscles, bones and blood data were corrected to their contributions to total body mass of mice. [80-83] Percent injected dose per gram organ was calculated for each body organs and fluids (%ID/g organ).

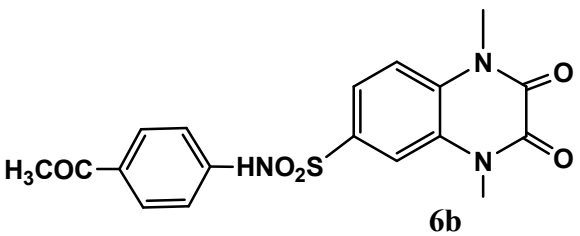

6b

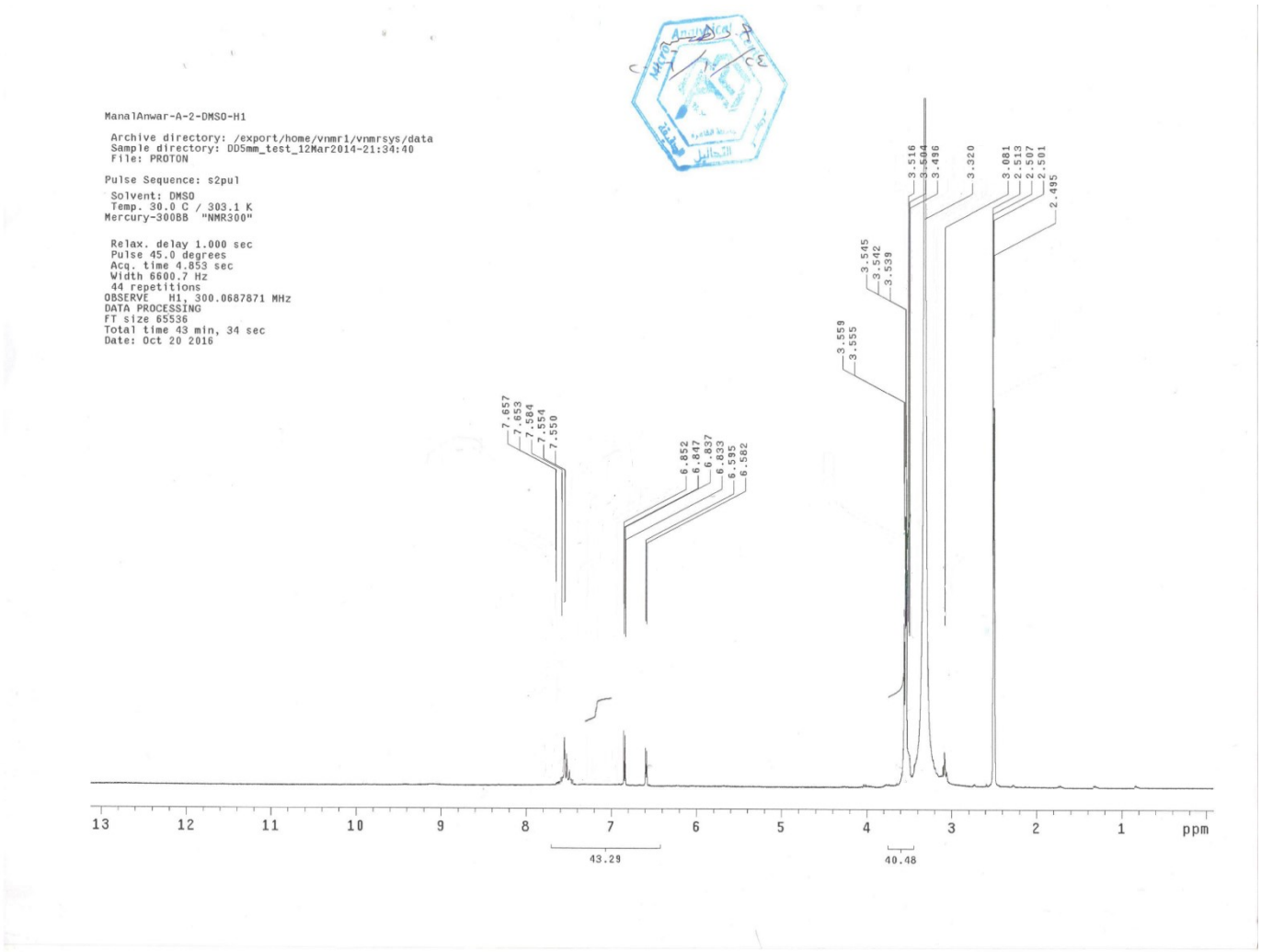

Figure S1. ^{1}H NMR spectrum of compound 6a

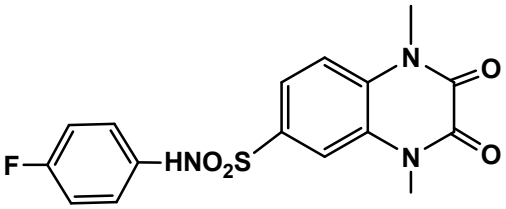

6d

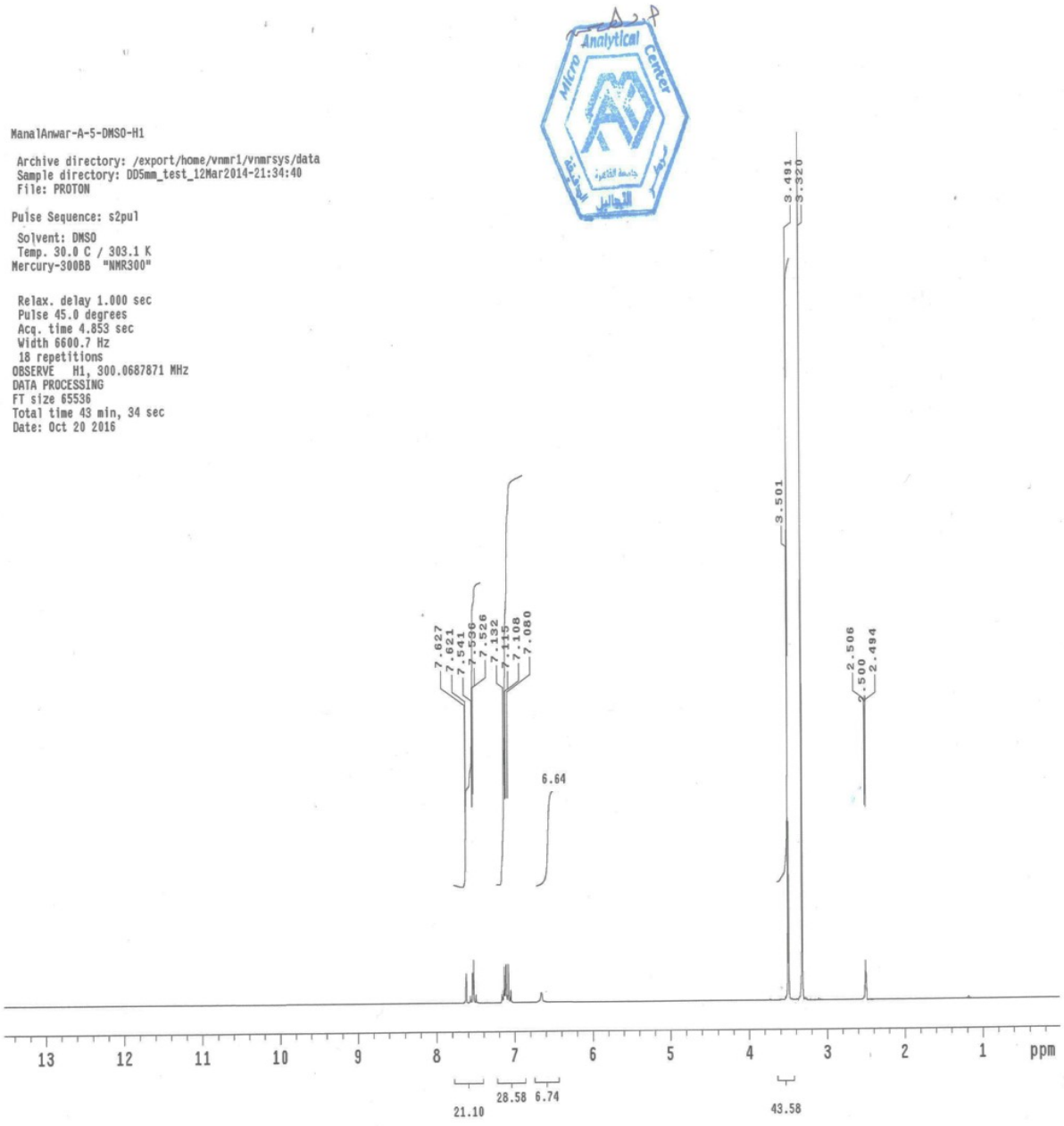

Figure S2. ^{1}H NMR spectrum of compound 6d

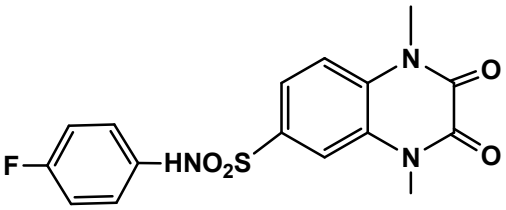

6d

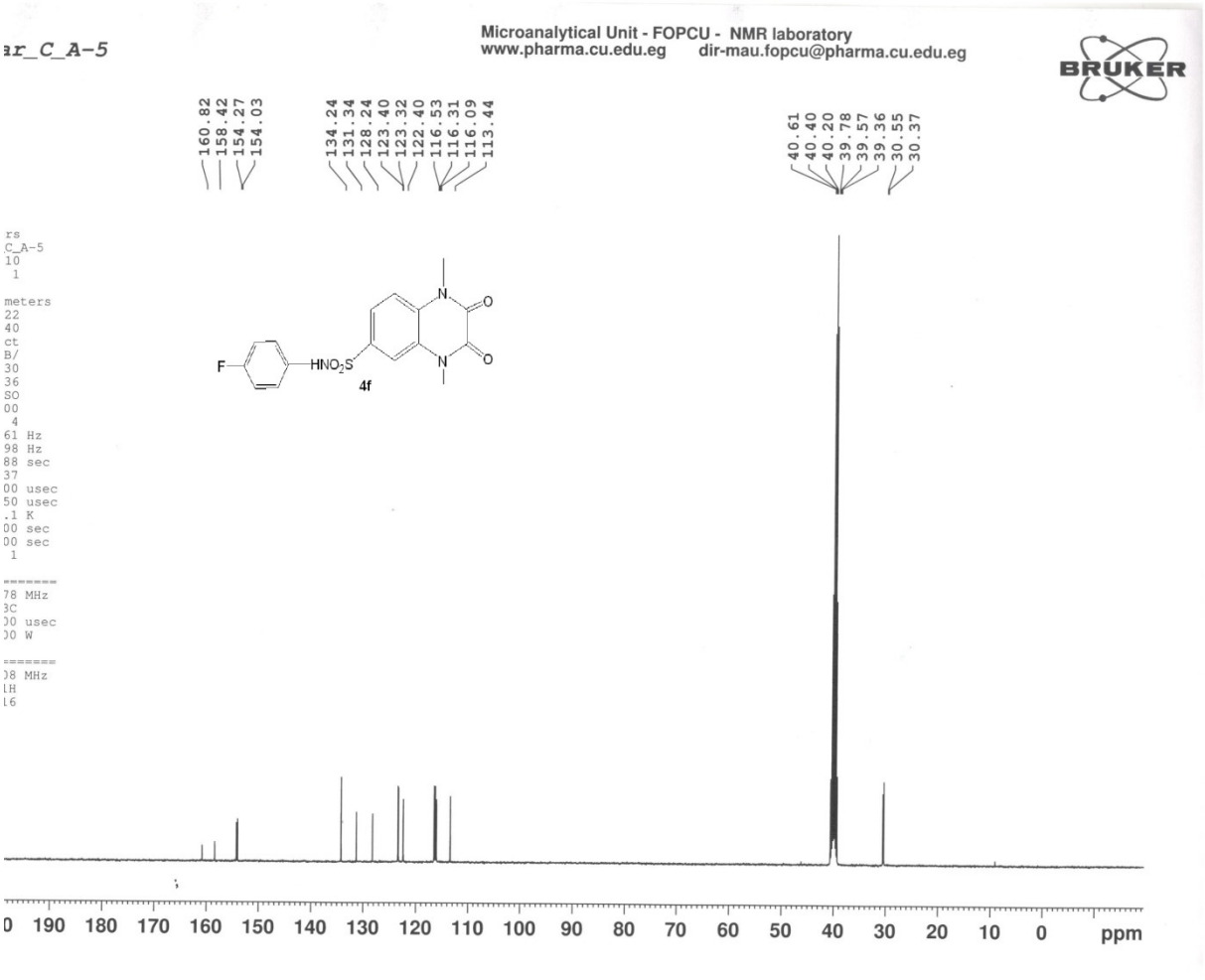

Figure S3. ^{13}C NMR spectrum of compound 6d

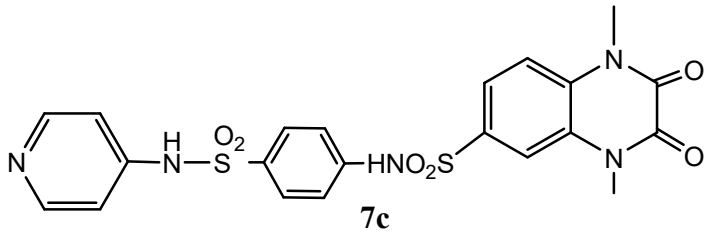

7c

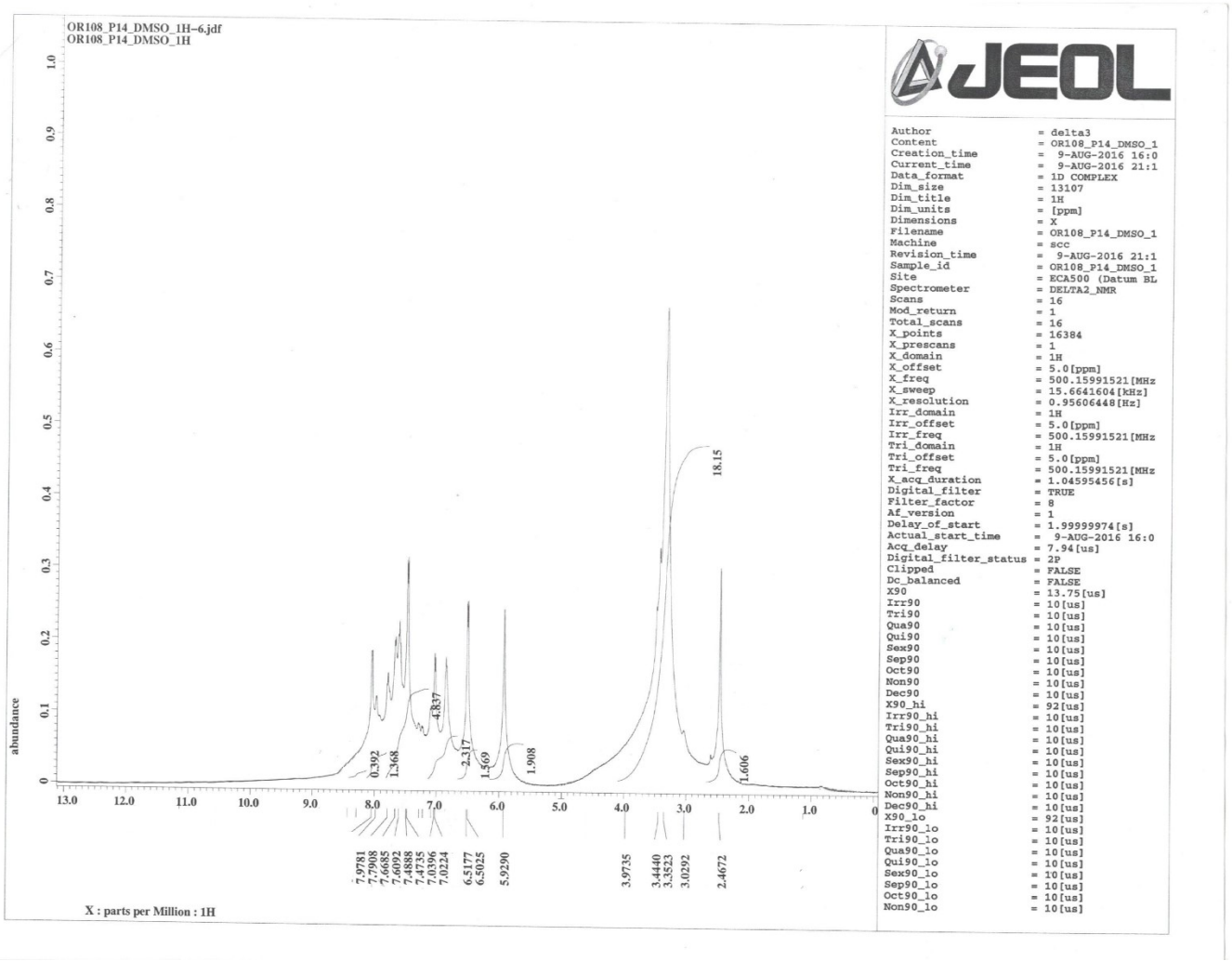

Figure S4. ^{1}H NMR spectrum of compound 7c

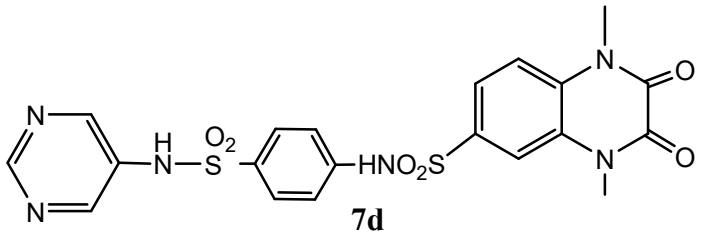

7d

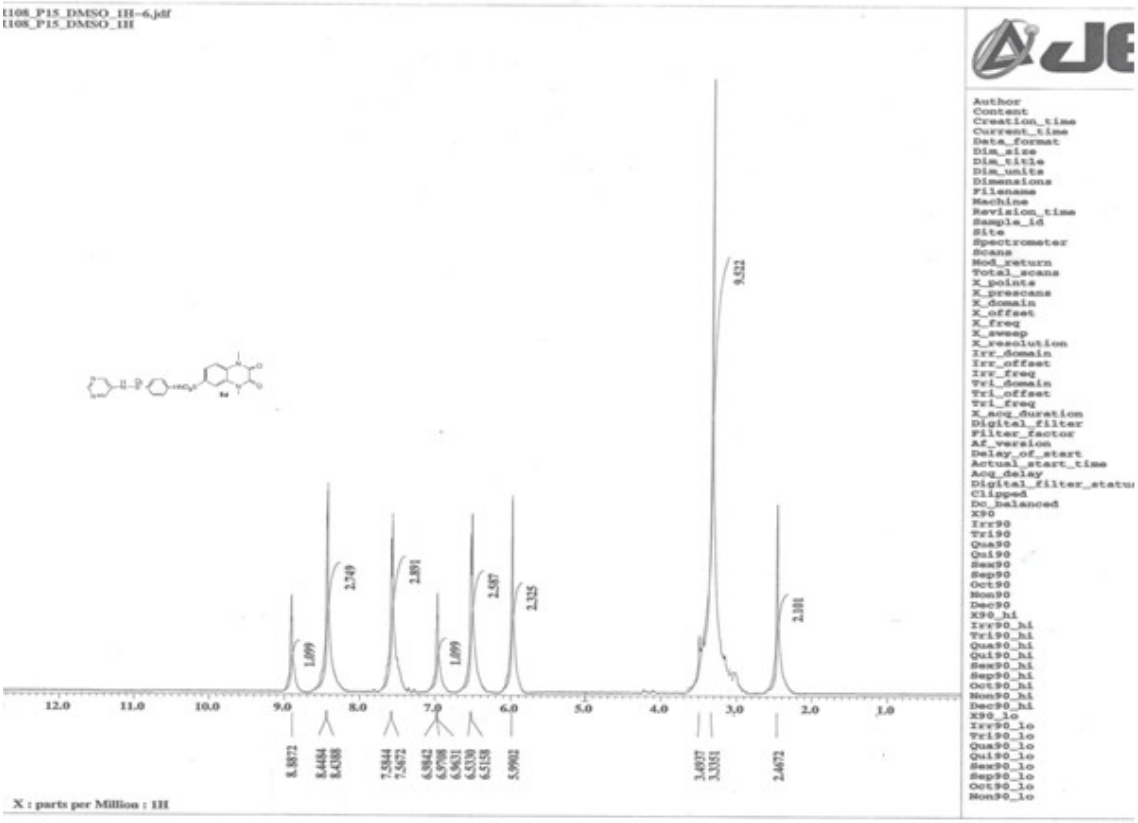

Figure S5. ^{1}H NMR spectrum of compound 7d

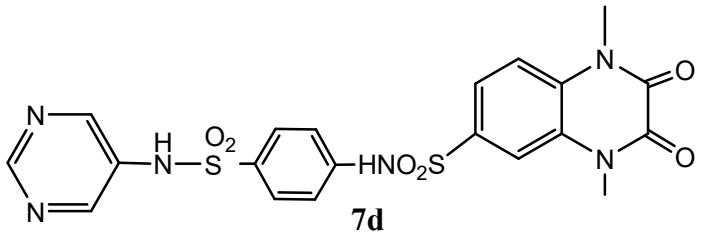

7d

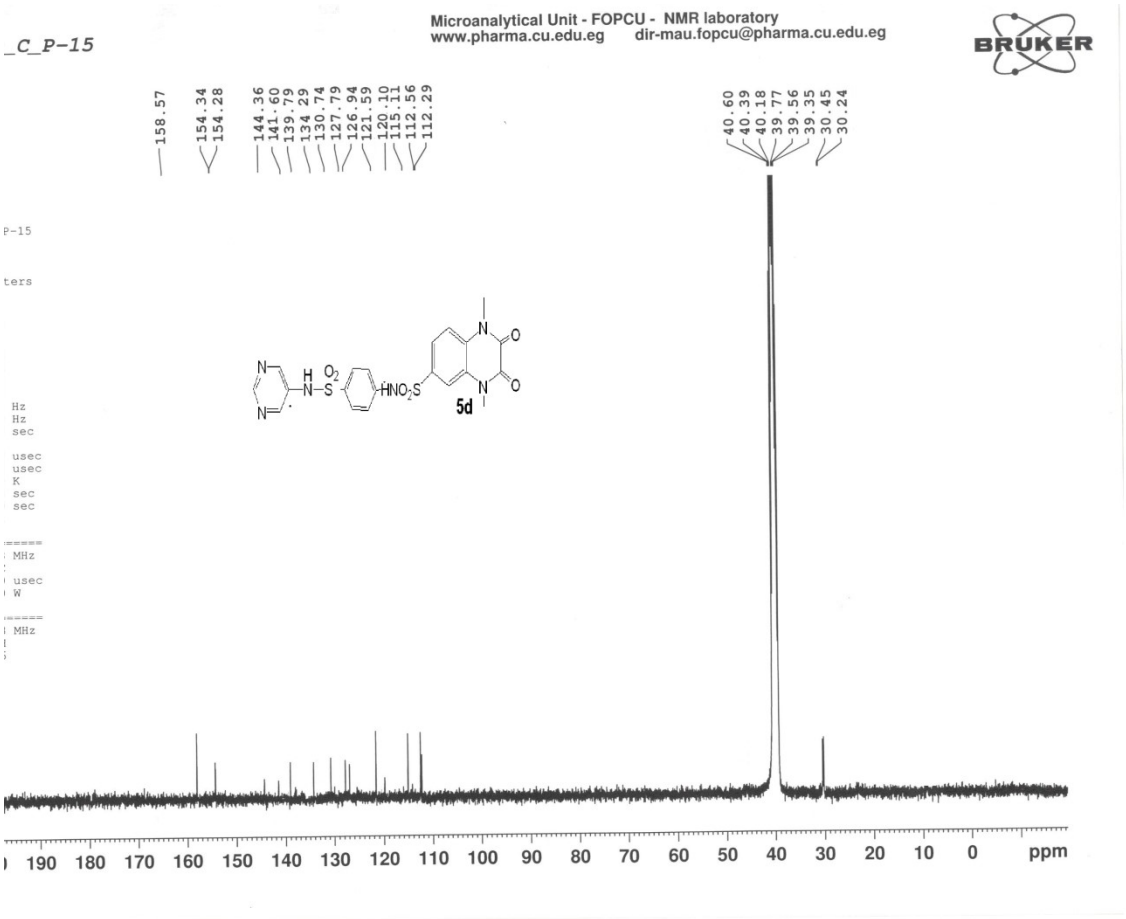

Figure S6. ^{13}C NMR spectrum of compound 7d

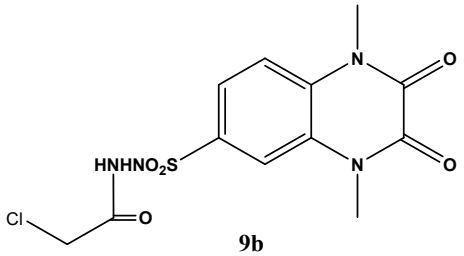

9b

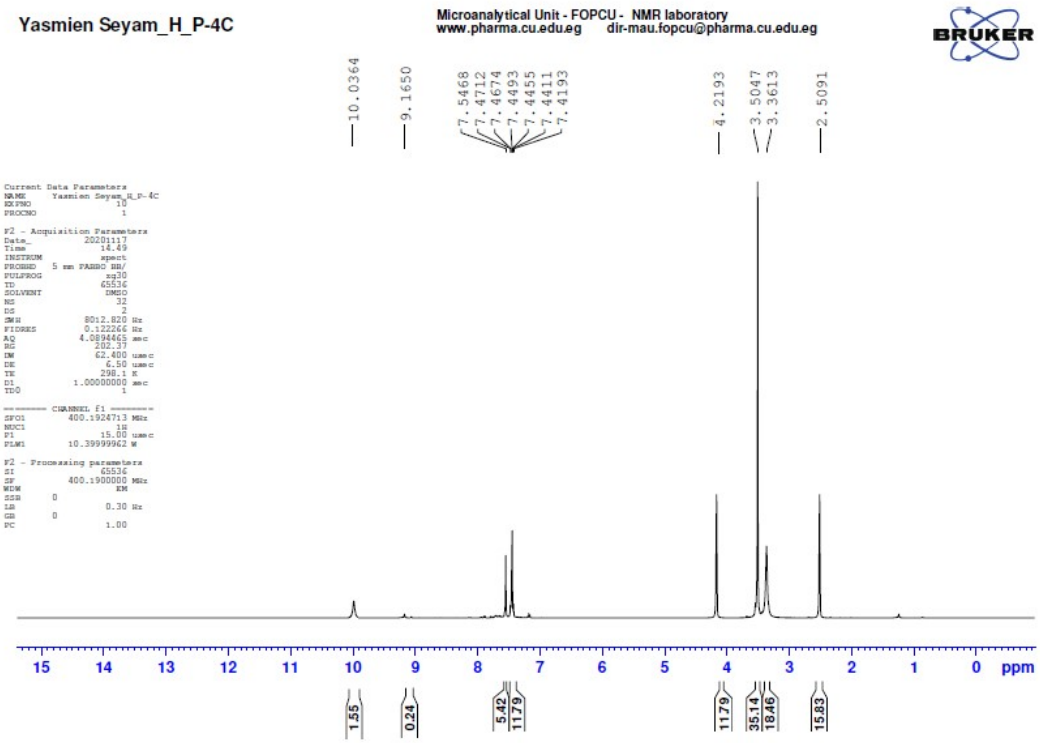

Figure S7. ^{1}H NMR spectrum of compound 9b

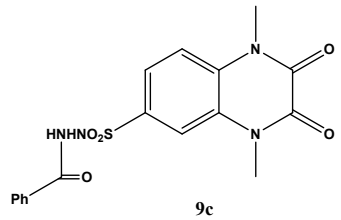

9c

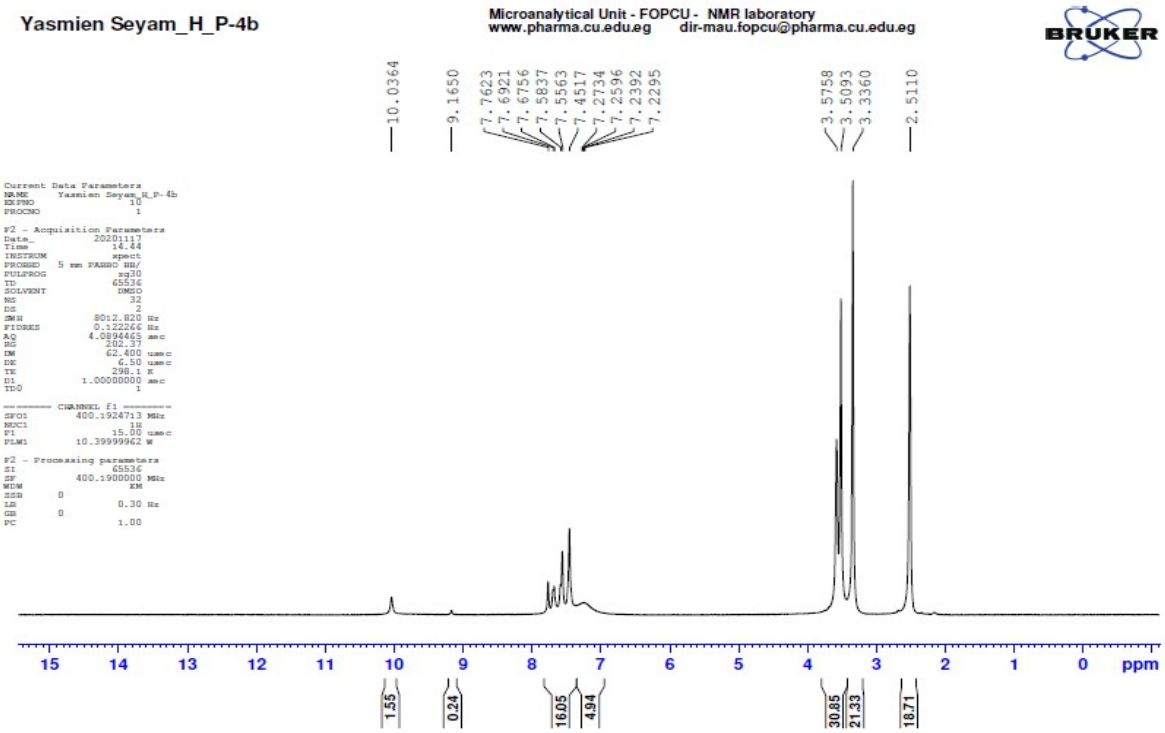

Figure S8. ^{1}H NMR spectrum of compound 9c

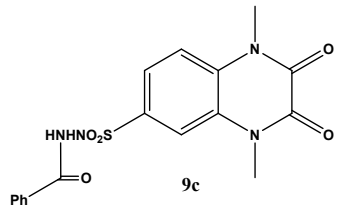

9c

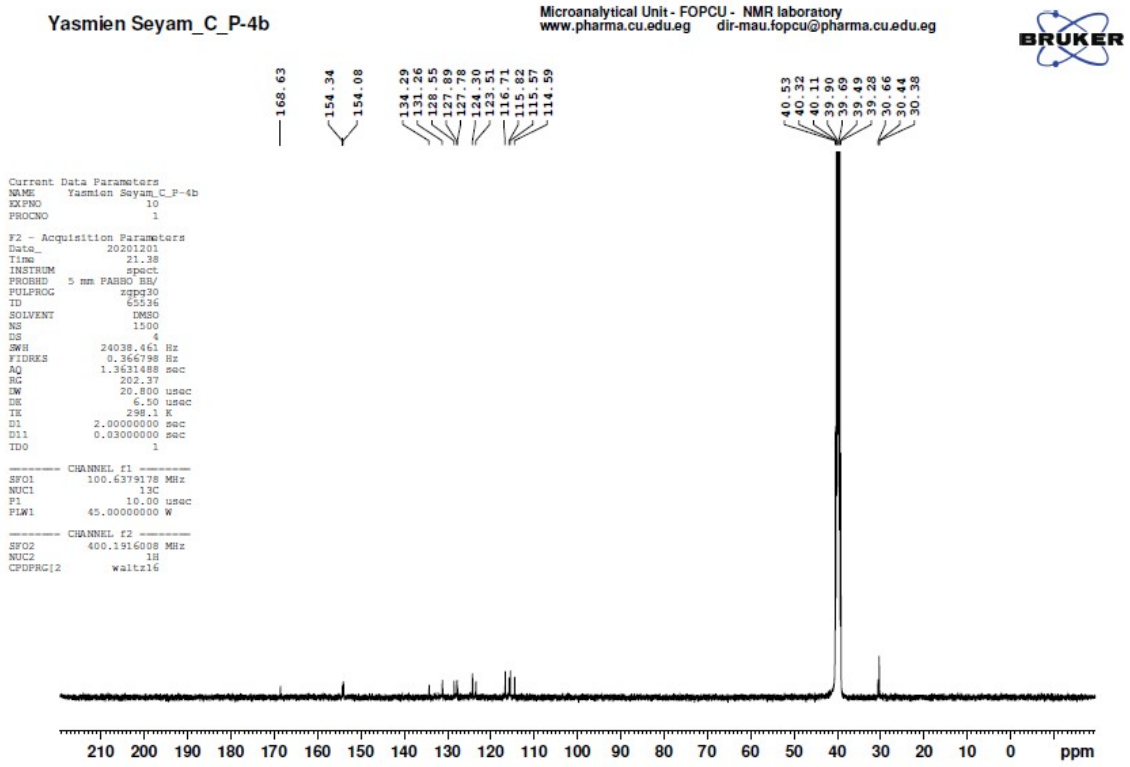

Figure S9. ^{13}C NMR spectrum of compound 9c

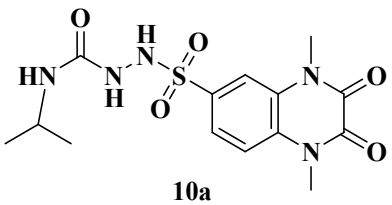

10a

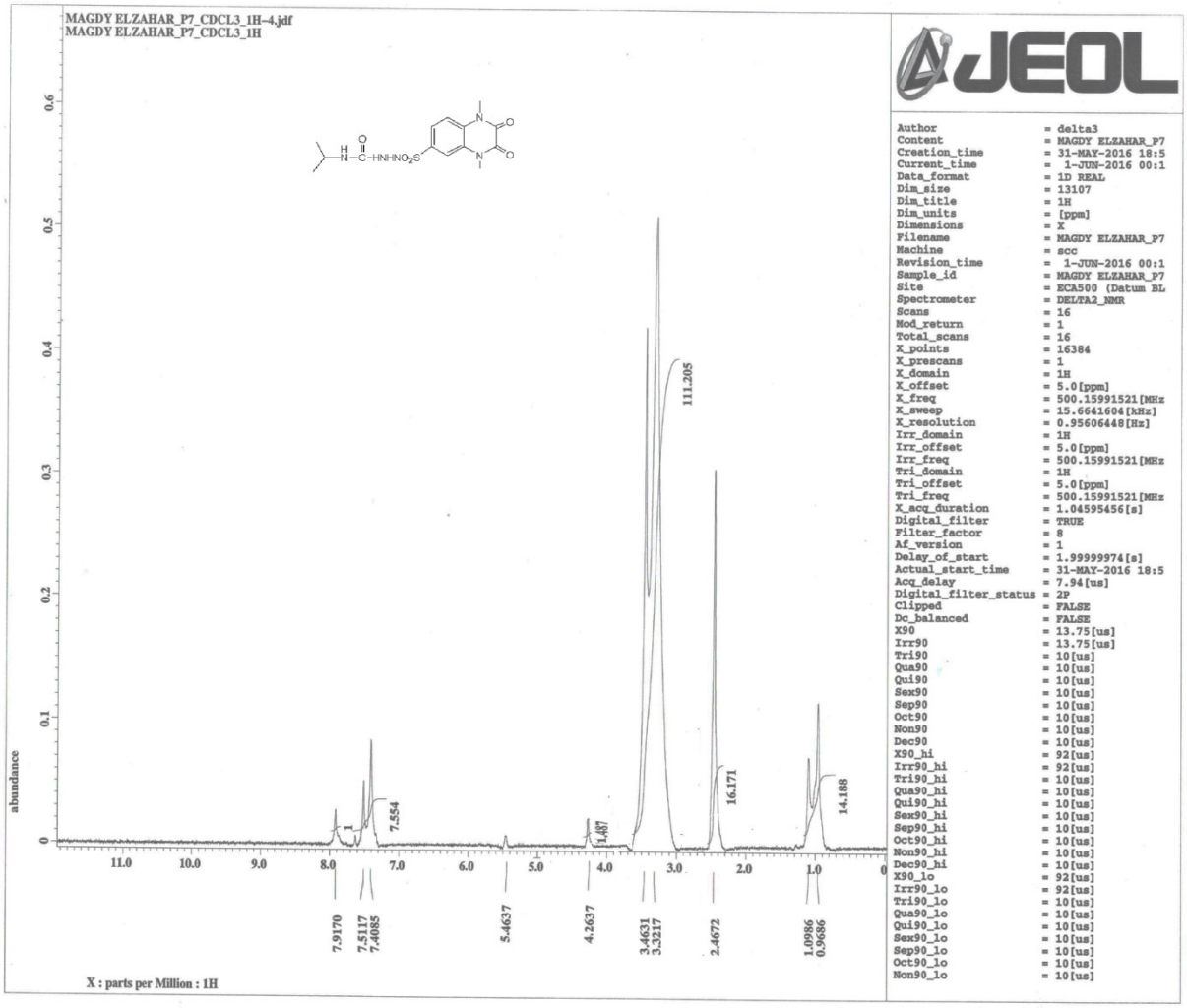

Figure S10. ^{1}H NMR spectrum of compound 10a

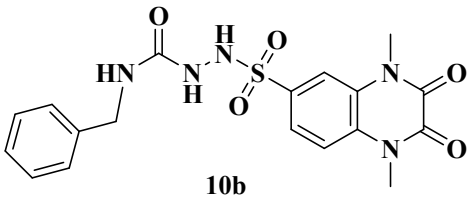

10b

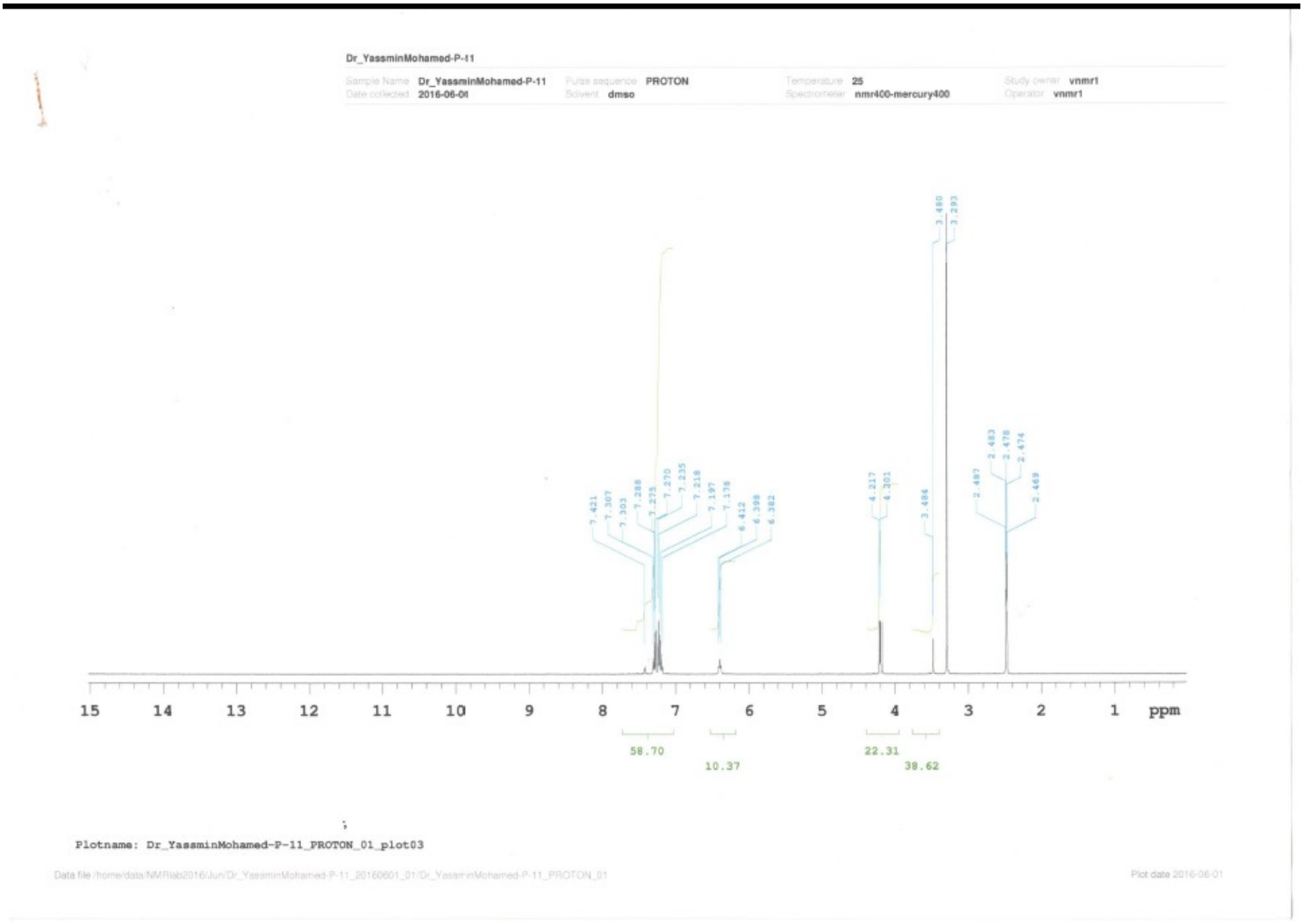

Figure S11. ^{1}H NMR spectrum of compound 10b

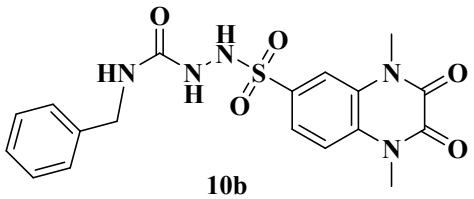

10b

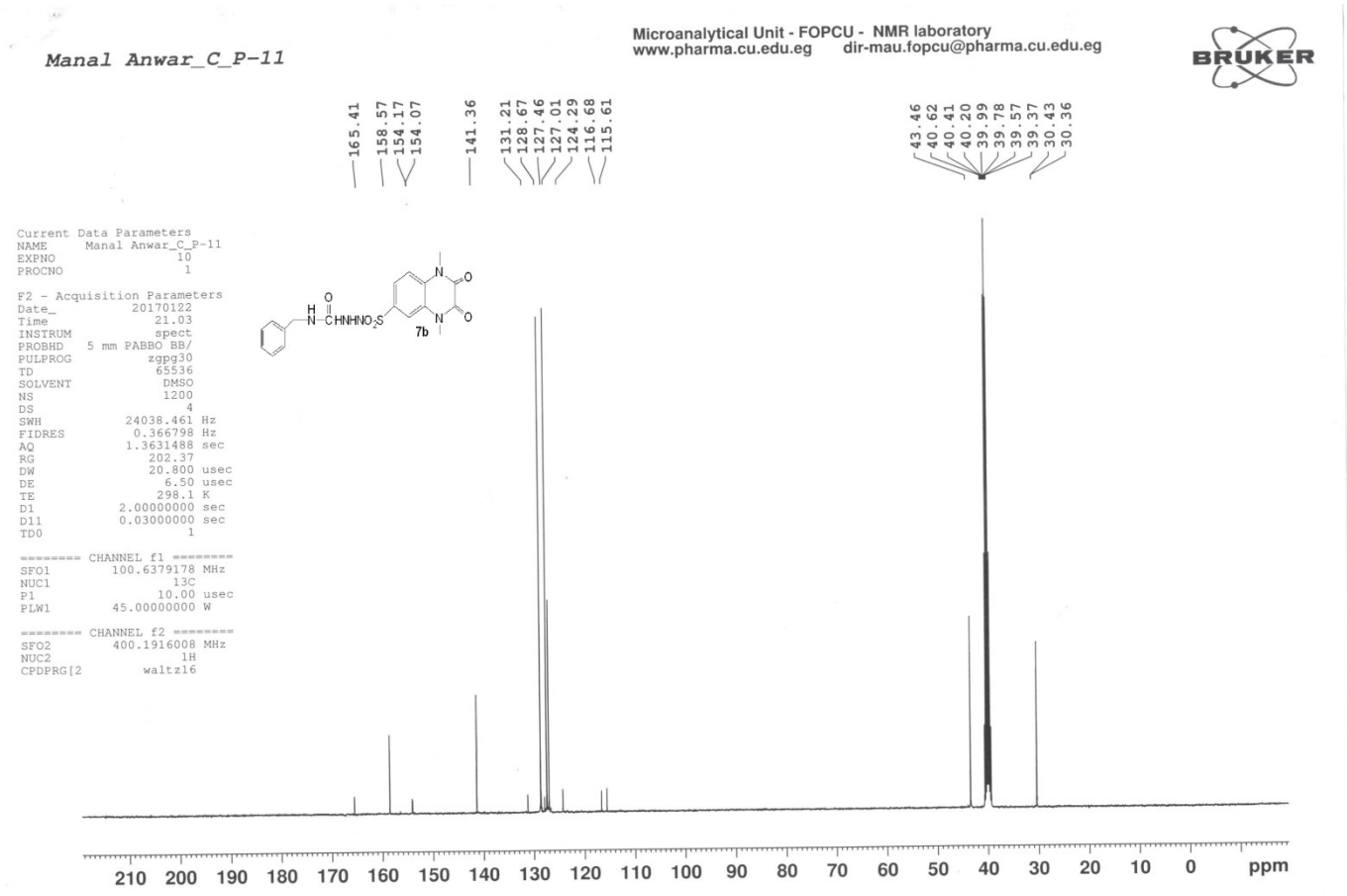

Figure S12. ^{13}C NMR spectrum of compound 10b

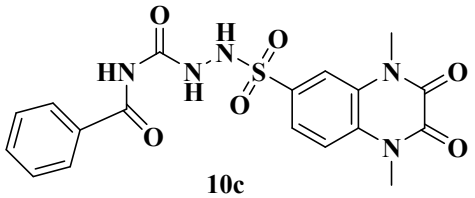

10c

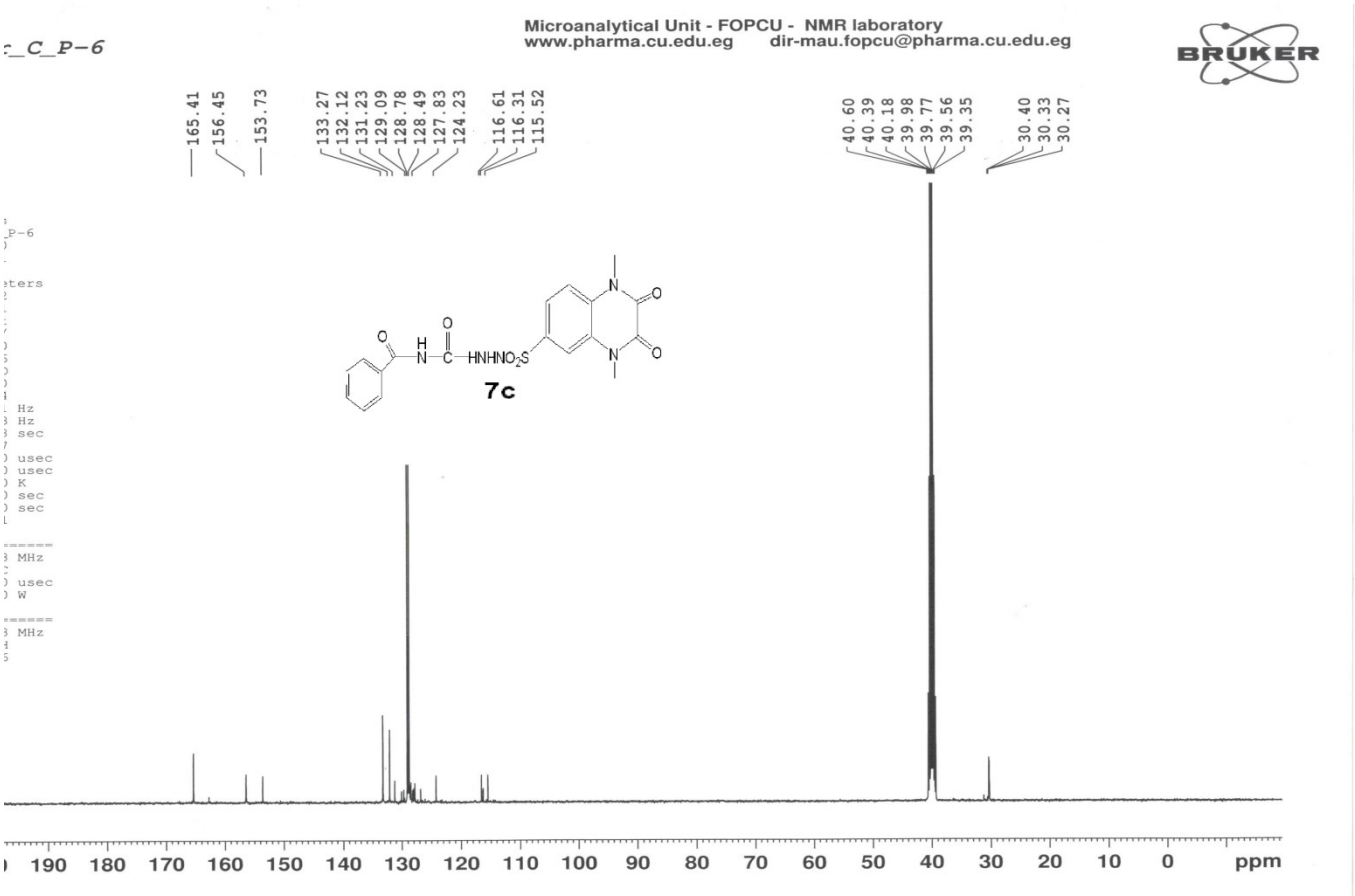
Microanalytical Unit - FOPCU - NMR laboratory
www.pharma.cu.edu.eg dir-mau.fopcu@pharma.cu.edu.eg
BRUKER
165.41
156.45
153.73
133.27
132.12
131.23
129.09
128.78
128.49
127.83
124.23
116.61
116.31
115.52
40.60
40.39
40.18
39.98
39.77
39.56
39.35
30.40
30.33
30.27
7c
190 180 170 160 150 140 130 120 110 100 90 80 70 60 50 40 30 20 10 0 ppm

Figure S13. ^{13}C NMR spectrum of compound 10c

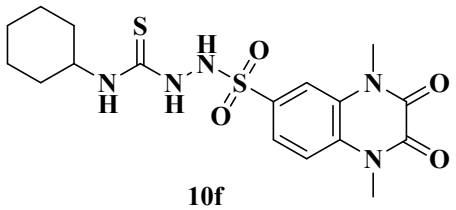

10f

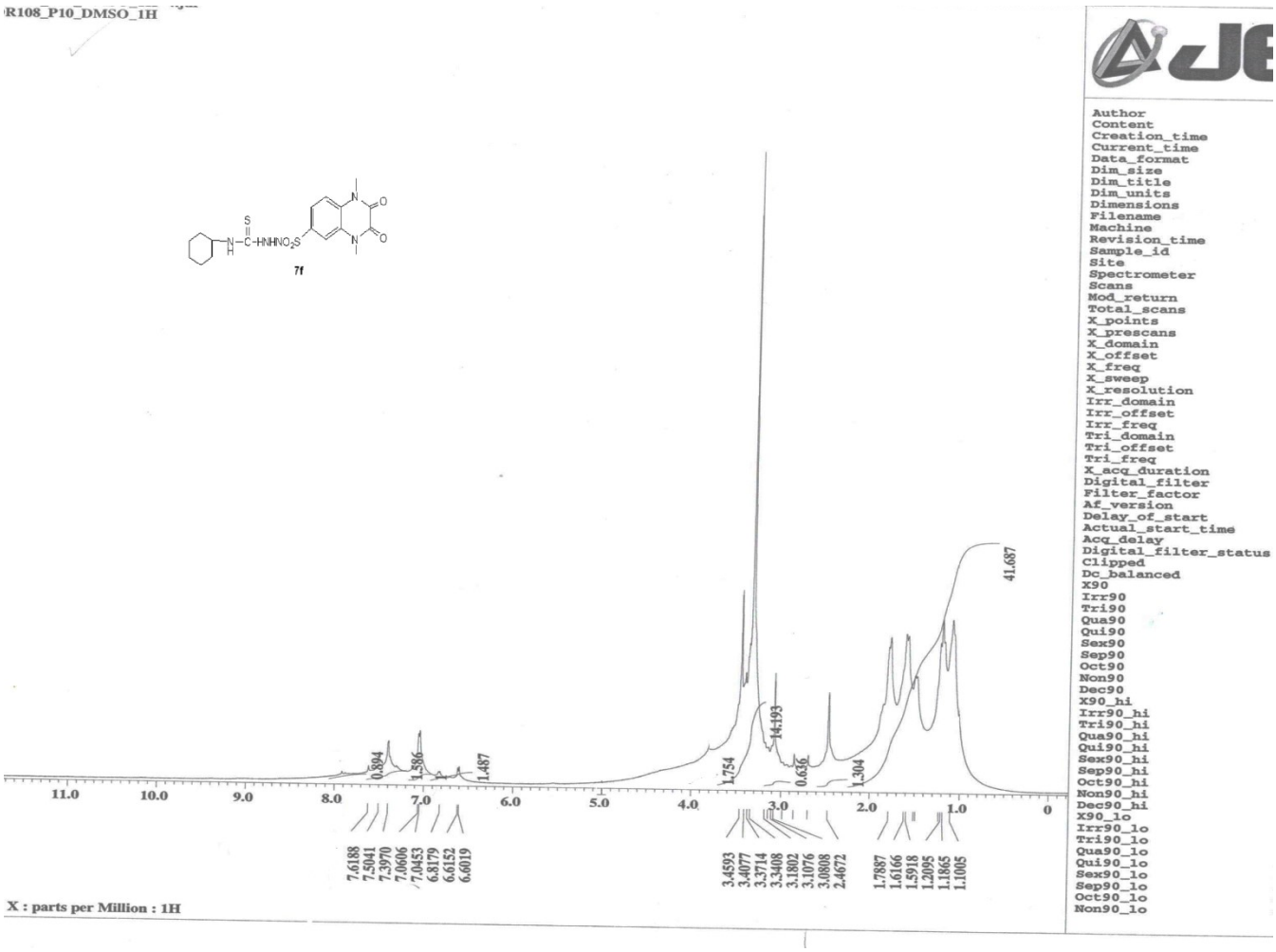

Figure S14. ^{1}H NMR spectrum of compound 10f

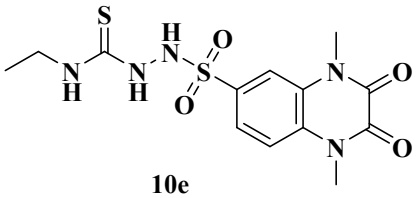

10e

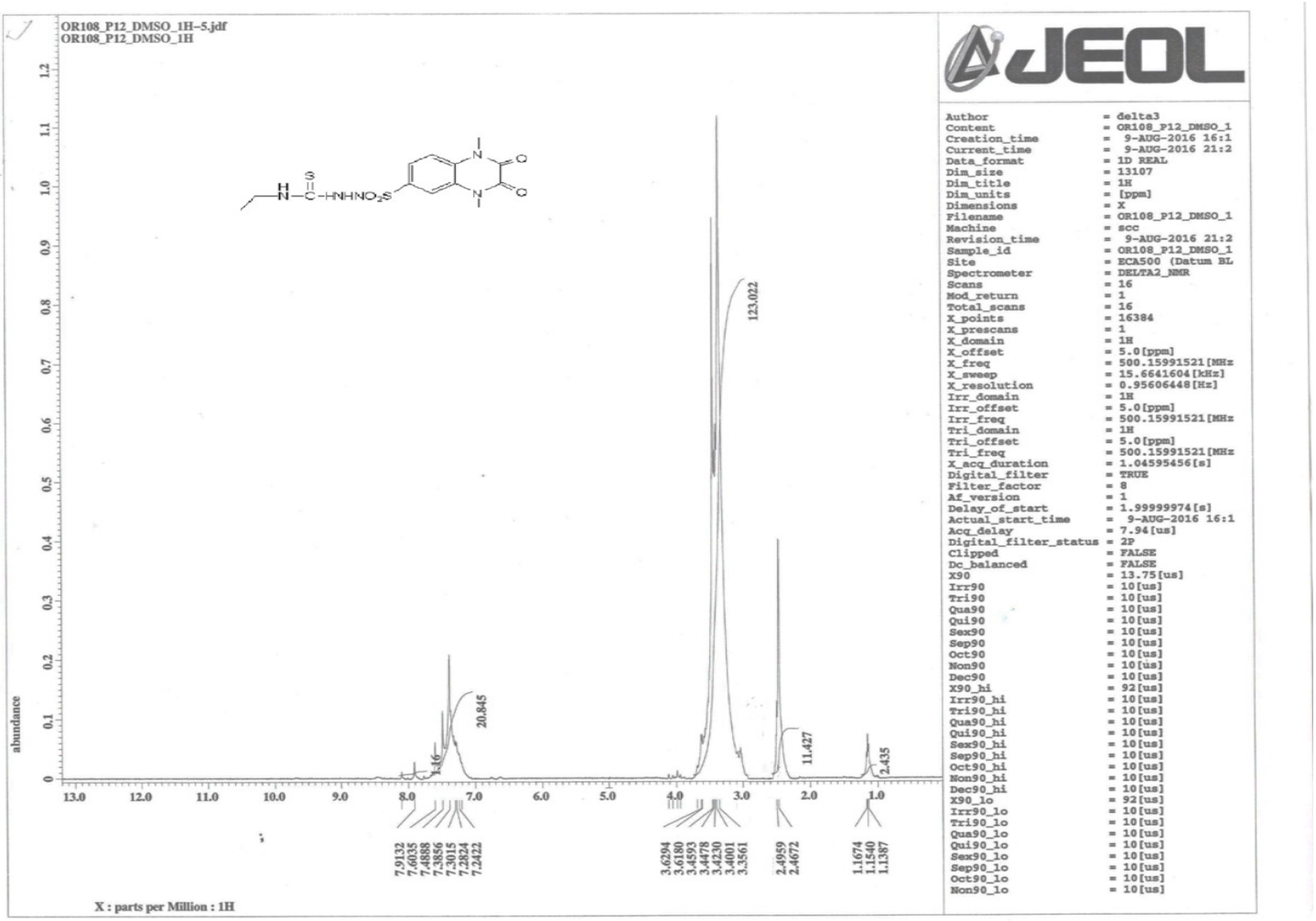

Figure S15. ^{1}H NMR spectrum of compound 10e

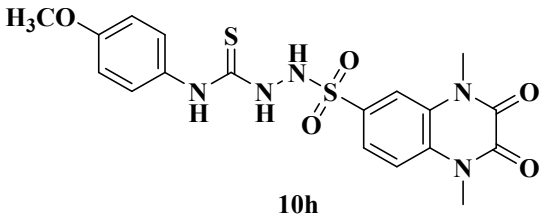

10h

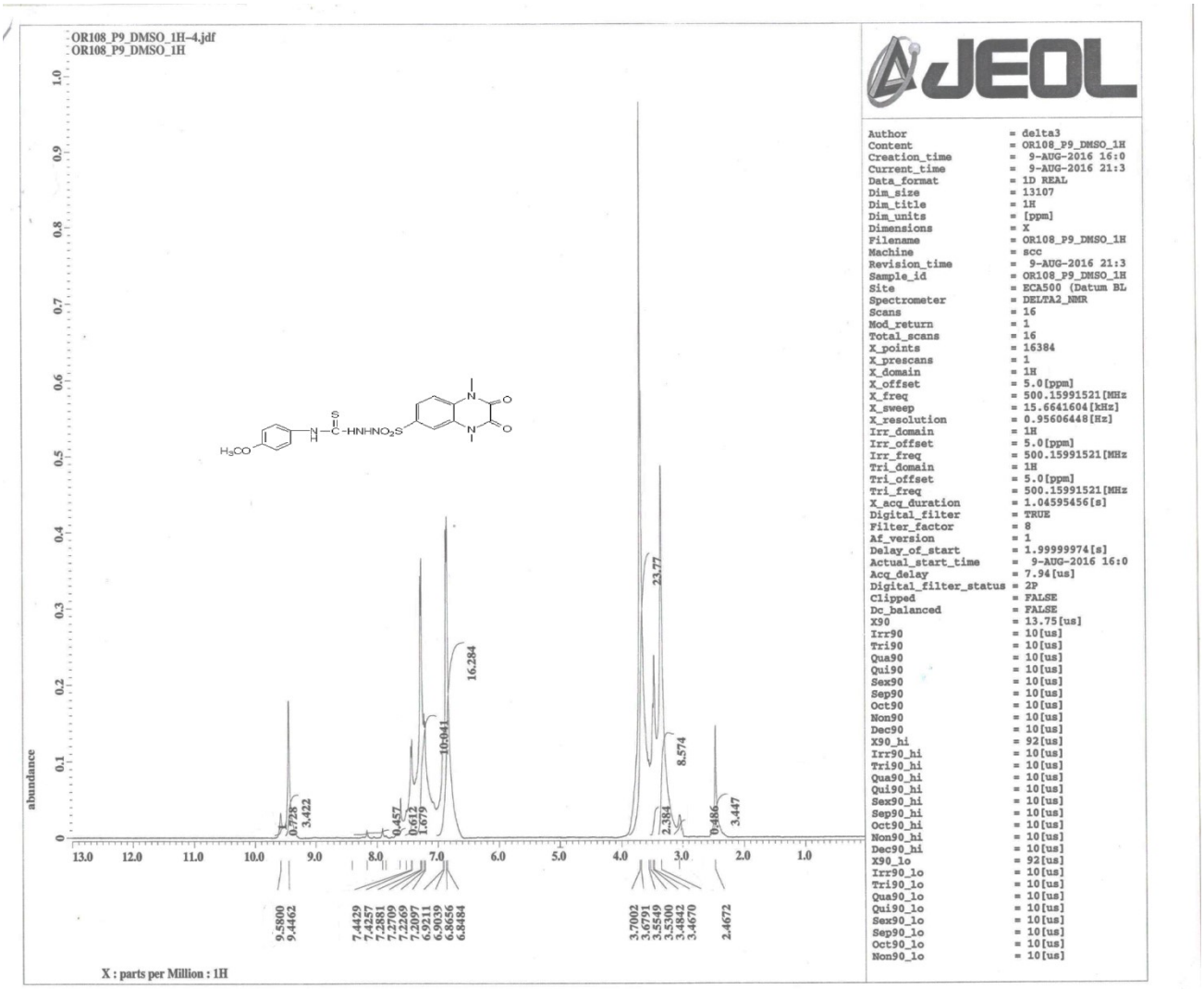

Figure S16. ^{1}H NMR spectrum of compound 10h